width is of little importance. The possibility of shifting the free-running frequency (through varactor tuning) in approximate synchronization with the change in frequency of the injected signal has not been investigated for subharmonic injection locking in this paper; with such a method, injection locking would provide only a part of the locking mechanism and locking bandwidth could be increased. The theory presented in this paper would be valid for that part of the locking that can be attributed to injection locking.

References

[1] H. G. Oltman and C. H. Nonnemaker, "Subharmonically injection phase-locked Gunn oscillator experiments," *IEEE Trans. Microwave Theory Tech.* (Corresp.), vol. MTT-17, pp. 728–729, Sept. 1969.

[2] C. H. Chien and G. C. Dalman, "Subharmonically injected phase-locked oscillator experiments," *Electron. Lett.*, vol. 6, pp. 240–241, Apr. 1970.

[3] R. Perichon, "Frequency-modulation noise of subharmonically injection phase-locked IMPATT oscillator," *IEEE Trans. Microwave Theory Tech. (Special Issue on Microwave Circuit Aspects of Avalanche-Diode and Transferred Electron Devices)* (Corresp.), vol. MTT-18, pp. 988–989, Nov. 1970.

[4] R. Adler, "A study of locking phenomena in oscillators," *Proc. IRE*, vol. 34, pp. 351–357, June 1946.

[5] K. Daikoku and Y. Mizushima, "Properties of injection locking in the nonlinear oscillator," *Int. J. Electron.*, vol. 31, pp. 279–292, 1971.

[6] A. L. Cullen, private communication.

[7] I. Markowski, "Fundamental and harmonic locking phenomena in negative resistance oscillators," Dep. Electron. Elec. Eng., Univ. College, London, England, Res. Rep.

[8] L. Gustafsson, G. H. B. Hansson, and K. I. Lundström, "On the use of describing functions in the study of nonlinear active microwave circuits," *IEEE Trans. Microwave Theory Tech.*, vol. MTT-20, pp. 402–409, June 1972.

[9] T. Berceli, "Output power of tunnel diode oscillators with harmonic frequency load," in *Proc. 8th Int. Conf. Microwaves and Optical Generation and Amplification* (Amsterdam, The Netherlands), 1970, pp. 10-25–10-30.

[10] A. Gelb and W. E. van der Velde, *Multiple Input Describing Functions and Nonlinear System Design.* New York: McGraw-Hill, 1968.

[11] B. Hansson and I. Lundström, "Phase locking of negative conductance oscillators," in *Proc. 1971 European Microwave Conf.* (Stockholm, Sweden), pp. A6/4:1–4.

[12] G. H. B. Hansson and K. I. Lundström, "Stability criteria for phase-locked oscillators," *IEEE Trans. Microwave Theory Tech.*, vol. MTT-20, pp. 641–645, Oct. 1972.

[13] G. C. Dalman, C. A. Lee, and C. Chien, "Noise in pulsed and CW solid-state microwave oscillators," in *Proc. 3rd Biennial Cornell Electrical Engineering Conf.* (Cornell Univ., Ithaca, N. Y.), 1971, pp. 175–182.

[14] L. Gustafsson and I. Lundström, to be published.

[15] M. Gilden and M. E. Hines, "Electronic tuning effects in the Read microwave avalanche diode," *IEEE Trans. Electron Devices (Special Issue on Semiconductor Bulk-Effect and Transit-Time Devices)*, vol. ED-13, pp. 169–175, Jan. 1966.

[16] J. G. Josenhans and T. Misawa, "Experimental characterization of a negative-resistance avalanche diode," *IEEE Trans. Electron Devices (Special Issue on Semiconductor Bulk-Effect and Transit-Time Devices)* (Corresp.), vol. ED-13, pp. 206–208, Jan. 1966.

[17] M. R. Spiegel, *Mathematical Handbook of Formulas and Tables.* New York: McGraw-Hill, 1968.

Microstrip Dispersion Model

WILLIAM J. GETSINGER

Abstract—**The assumption that the quasi-TEM mode on microstrip is primarily a single longitudinal-section electric (LSE) mode leads to a transmission line model whose dispersion behavior can be analyzed and related to that of microstrip. Appropriate approximations yield simple, closed-form expressions that allow slide-rule prediction of microstrip dispersion.**

Nomenclature

a, a', b, b', s, w	Mechanical dimensions of conventional microstrip and the LSE mode model (Fig. 2).
c	Speed of light in free space = 11.8 in/ns.
C'	Capacitance per unit length of microstrip line at zero frequency.
D	Width of the zero-frequency parallel-plate microstrip equivalent structure.
f	Frequency.
f_i	Frequency of inflection of the dispersion curve.
f_p	Parameter of the dispersion function.
G	Empirical parameter used to simplify the microstrip dispersion function.
k_0	Free-space wavenumber.
L'	Inductance per unit length of microstrip line at zero frequency.
Z_f	Microstrip characteristic impedance at frequency f.
Z_0	Microstrip characteristic impedance at zero frequency.
γ	Propagation constant along the microstrip line.
γ_a	Transverse propagation constant in the air-filled part of the microstrip model.
γ_s	Transverse propagation constant in the dielectric-filled part of the microstrip model.
ϵ_e	Microstrip effective dielectric constant (a function of frequency).
ϵ_{ei}	Microstrip effective dielectric constant at the inflection point.
ϵ_{e0}	Microstrip effective dielectric constant at zero frequency.
ϵ_0	Permittivity of free space = 8.85×10^{-12} F/m.
ϵ_s	Substrate relative dielectric constant.
η_0	Impedance of free space = 376.7 Ω.
μ_0	Permeability of free space = 31.92 nH/in, or $4\pi \times 10^{-7}$ H/m.
ω	Radian frequency.

Manuscript received April 13, 1972; revised July 10, 1972. This paper is based upon work performed at COMSAT Laboratories under Corporate sponsorship.

The author is with COMSAT Laboratories, Clarksburg, Md. 20734.

Introduction

PROPAGATION on microstrip is usually handled as though the line were filled with dielectric and carried a TEM mode. This is an adequate representation except that the effective dielectric constant changes slowly with frequency, making microstrip dispersive [1].

Both analytical [2] and empirical [3], [4] attempts to describe microstrip dispersion have been published. (A good bibliography is given in [4].) The analytical techniques have been nearly exact, but have required numerical solution on large electronic computers. Thus these techniques have been too ponderous for practical engineering application. The empirical techniques, on the other hand, have had limited ranges of applicability and inadequate theoretical foundations for confidence in application.

With the intention of achieving analytical simplicity, this paper considers microstrip propagation as a single longitudinal-section electric (LSE) [5] mode. Physical reasoning indicates that this might be a practical approximation for investigating dispersion on microstrip. However, the structure of microstrip precludes analysis by direct means. Thus a structure (the model) has been conceived that resembles microstrip in all but shape, but whose LSE-mode propagation can be analyzed directly. It is assumed that the propagation characteristics (dispersion) of the model can be applied to microstrip by appropriate adjustment of parameters.

Since it does not follow from theory that the dispersion functions of the two structures must be the same, as it does for differently shaped, homogeneously filled waveguides, the validity of the model must be tested by its agreement with measured dispersion of actual microstrip.

It turns out that the model yields a simple closed-form algebraic expression that closely describes measured dispersion in microstrip. It is found that only one parameter in addition to those available from static analyses of microstrip, such as the MSTRIP program [6], is necessary to describe microstrip dispersion.

For convenience, the results of this paper are illustrated in Fig. 1. The symbols are defined in the Nomenclature list. The dispersion relationships shown in Fig. 1 have been found to agree with a theoretical prediction [2] based on coupled integral equations, with published [1] measurements of a 20-Ω microstrip line on a rutile ($\epsilon_s = 104$) substrate and with measurements on 0.025- and 0.050-in alumina ($\epsilon_s \approx 10$) substrates.

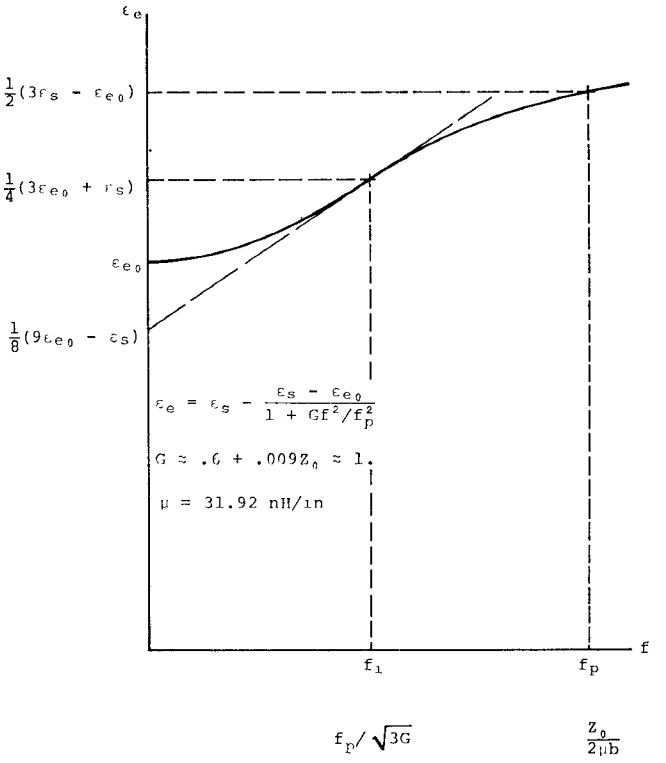

Fig. 1. Microstrip dispersion relationships.

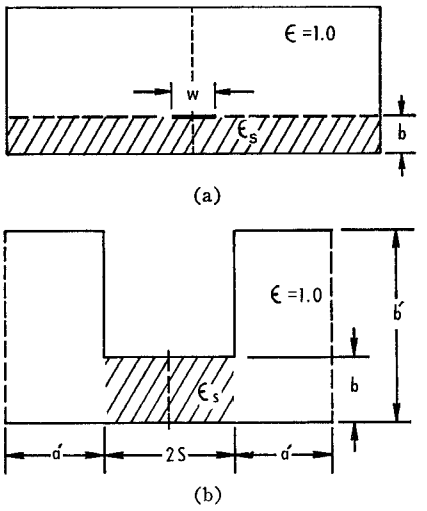

Fig. 2. (a) Conventional microstrip. (b) LSE model for microstrip.

The Analytical Model

A conventional microstrip structure is shown in Fig. 2(a). The fields are concentrated around the edges of the strip and in the dielectric beneath the center strip. Near the strip edges, the magnetic field is predominantly normal to and the electric field predominantly tangential to the air–dielectric interface. This is characteristic of the LSE mode [5], [7]. The structure of Fig. 2(a) is intractable to direct analysis on this basis, but its boundaries can be distorted to result in a model, shown in Fig. 2(b), that can be analyzed.

The electric field lines emanating from the lower surface of the center strip of the microstrip in Fig. 2(a) pass only through the substrate dielectric, as do the electric field lines emanating from the center portion of the model of Fig. 2(b). The electric fields emanating from the upper surface of the center strip of the microstrip occupy a much larger space, which is mostly filled with air. This space is approximated by the large, air-filled end sections of the model. The magnetic wall (indicated by a dashed line) above the center strip of Fig. 2(a) is split and the upper wall of the center strip is unfolded at the edge, stretched out, and bent to form the end-section boundaries of Fig. 2(b). Thus the model consists of one parallel-plate transmission line, which has a dielectric constant ϵ_s, width $2s$, and height b, connected without junction effect to other parallel-plate transmission lines that have a dielectric constant of one, width a', and height b'.

The heuristic assumption made is that because the two regions, air filled and dielectric filled, of the model and the microstrip are grossly similar, the two structures will have the same dispersion behavior for the same mode of propagation. It is clear that junction capacitance could be included at the steps of the model to make it more realistic, or more

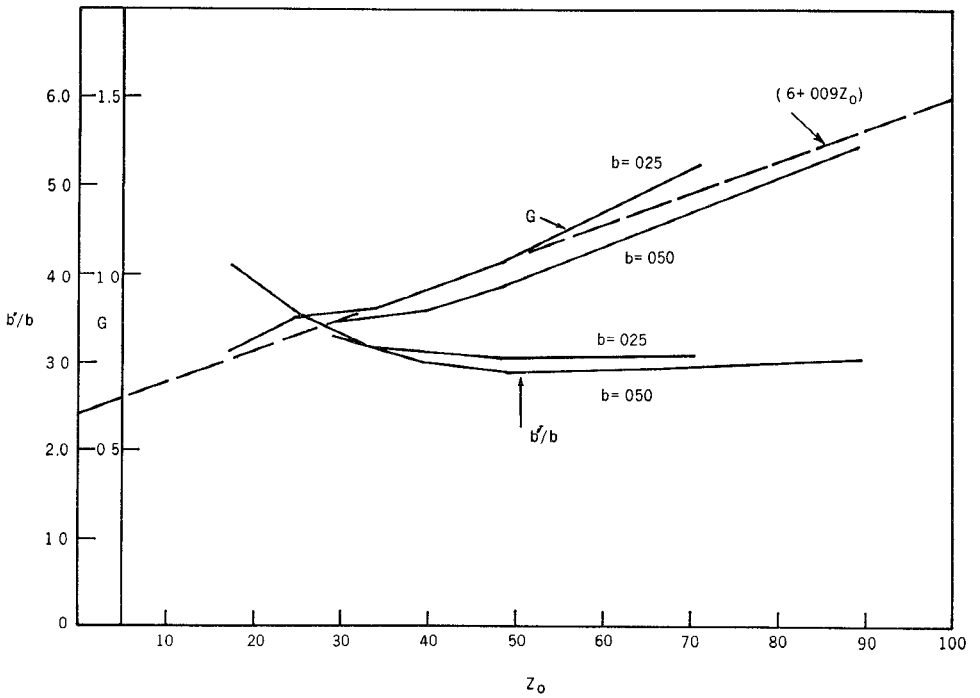

Fig. 3. Microstrip dispersion parameters.

like microstrip, but this would greatly complicate the analysis and has not been found necessary for practical results.

The model is, after all, only an intuitive aid in setting up the simplest mathematics that lead to a useful dispersion relation; it need not be physically realizable.

The analysis proceeds by forcing the model to have the same electrical characteristics at zero frequency as the microstrip. (These characteristics can be found from well-known and widely available computer programs, such as MSTRIP [6].) Next, a transverse resonance analysis of the model relates the propagation constant (or effective dielectric constant) to frequency. A closed-form approximation of this function is then found and compared with measured microstrip dispersion to determine the unknown parameter b'/b [see Fig. 2(b)]. Finally, the results show that b'/b and related parameters are nearly constant or linear with characteristic impedance. Hence, it is possible to derive simple formulas that can be used to predict the dispersion of microstrip transmission lines.

Zero-Frequency Relationships

A static analysis such as the MSTRIP program [6] is employed to yield the effective relative dielectric constant ϵ_{e0} and the characteristic impedance Z_0 for given w/b, ϵ_s, and possibly other dimensional parameters, such as strip thickness or proximity of an upper ground plane. [See Fig. 2(a).]

The inductance L' and capacitance C' per unit length of the microstrip can be written as

$$\frac{L'}{\mu_o} = \frac{Z_0}{\eta_o}\sqrt{\epsilon_{e0}} \tag{1a}$$

$$\frac{C'}{\epsilon_o} = \frac{\eta_o\sqrt{\epsilon_{e0}}}{Z_0} \tag{1b}$$

respectively, where

$$\eta_o = \sqrt{\frac{\mu_o}{\epsilon_o}} = 376.7\ \Omega. \tag{2}$$

The subscript o indicates free-space values of the constitutive parameters, while the subscript 0 indicates zero-frequency values of the characteristic impedance and effective dielectric constant.

Inductance and capacitance per unit length for the LSE model [Fig. 2(b)] at zero frequency can be written as

$$\frac{L'}{\mu_o} = \frac{1}{2[(a'/b') + (s/b)]} \tag{3a}$$

$$\frac{C'}{\epsilon_o} = 2\left(\frac{a'}{b'} + \epsilon_s\frac{s}{b}\right) \tag{3b}$$

respectively. Equating equivalent parameters yields

$$\frac{a'}{b'} = \frac{\eta_o}{2Z_0\sqrt{\epsilon_{e0}}}\cdot\frac{\epsilon_s - \epsilon_{e0}}{\epsilon_s - 1} \tag{4a}$$

$$\frac{s}{b} = \frac{\eta_o}{2Z_0\sqrt{\epsilon_{e0}}}\cdot\frac{\epsilon_{e0} - 1}{\epsilon_s - 1}. \tag{4b}$$

Transverse Resonance Solution

The sum of the admittances on the left and right of either air–dielectric interface of Fig. 2(b) must equal to zero according to the transverse resonance [5], [7] technique. The propagation constants are related by

$$\gamma_a^2 + \gamma^2 + k_o^2 = 0 \tag{5}$$

in the air-filled section and by

$$\gamma_s^2 + \gamma^2 + \epsilon_s k_o^2 = 0 \tag{6}$$

in the dielectric-filled section. In (5), (6), γ is the propagation constant along the transmission line and applies to both air-

and dielectric-filled sections, while γ_a is the constant in the transverse direction in the air-filled section and γ_s is the constant in the transverse direction in the dielectric-filled section. Finally,

$$k_o = \omega/c \tag{7}$$

is the free-space wave number.

The vertical dashed lines of Fig. 2(b) indicate magnetic walls or open-circuit boundaries. The characteristic admittances in the two sections are proportional to their propagation constants and inversely proportional to their heights. Thus the sum of the admittances at the interface is

$$\frac{\gamma_a}{b'} \tanh \gamma_a a' + \frac{\gamma_s}{b} \tanh \gamma_s s = 0. \tag{8}$$

The following approximation is used to solve the preceding transcendental equation:

$$\tanh x \approx \frac{1}{(1/x) + (x/3)}. \tag{9}$$

Equation (9) is in error by about 1.5 percent at $x=1$ rad. As an example of the range of applicability, $\gamma_s s = 1.0$ for a 25-Ω line on a 0.05-in alumina substrate at about 10 GHz. The use of higher impedances and thinner substrates raises the frequency at which an error of this magnitude occurs.

Substituting (9) into (8) yields

$$\frac{b'/a'}{\gamma_a{}^2} + \frac{b/s}{\gamma_s{}^2} = -\frac{a'b' + sb}{3} \tag{10}$$

after some manipulation.

The longitudinal propagation constant can be expressed in terms of the effective dielectric constant; i.e.,

$$\gamma^2 = -k_o{}^2 \epsilon_e. \tag{11}$$

Substituting (11) into (5) and (6) results in

$$\gamma_a{}^2 = k_o{}^2(\epsilon_e - 1) \tag{12}$$

$$\gamma_s{}^2 = -k_o{}^2(\epsilon_s - \epsilon_e). \tag{13}$$

Substituting (12) and (13) into (10) yields

$$\frac{b/s}{\epsilon_s - \epsilon_e} - \frac{b'/a'}{\epsilon_e - 1} = \frac{a'b' + sb}{3} k_o{}^2 \tag{14}$$

which is the basic dispersion relationship.

The unknown parameters a' and b' can be reduced to a single unknown by assuming that a is the solution of (4a) when b' is given the value of b, which is known. That is,

$$a' = a\left(\frac{b'}{b}\right) \tag{15}$$

where b'/b is the new unknown parameter. When (15) is substituted into (14), the basic dispersion relationship becomes

$$\frac{1/s}{\epsilon_s - \epsilon_e} - \frac{1/a}{\epsilon_e - 1} = \frac{a(b'/b)^2 + s}{3} k_o{}^2. \tag{16}$$

When (16) is solved for $\epsilon_s - \epsilon_e$ as the dependent variable, a quadratic results. Its solution is

$$\epsilon_s - \epsilon_e = \frac{B}{2}\left\{1 - \sqrt{1 - \frac{4(\epsilon_s - 1)/s}{B^2\left[\left\{[a(b'/b)^2 + s]/3\right\} k_o{}^2\right]}}\right\} \tag{17}$$

where

$$B = (\epsilon_s - 1) + \frac{(a+s)/as}{\left\{[a(b'/b)^2 + s]/3\right\} k_o{}^2} \tag{18}$$

and the negative root has been selected because it is physically meaningful.

Equation (17) can be simplified by observing that the second term under the radical is considerably less than one for practical cases and then by using the usual square-root approximation. (For a 25-Ω line on a 0.05-in alumina substrate at 12.5 GHz, the error is about 5 percent.) After a small amount of algebra, the result is

$$\epsilon_e = \epsilon_s - \frac{[(\epsilon_s - 1)a]/(a+s)}{1 + k_o{}^2(as/3)(\epsilon_s - 1)\left\{[a(b'/b)^2 + s]/(a+s)\right\}}. \tag{19}$$

Substituting (4) and (15) into (19) makes it possible to express (19) in terms of known quantities, except for the parameter b'/b; i.e.,

$$\epsilon_e = \epsilon_s - \frac{\epsilon_s - \epsilon_{e0}}{1 + G(f^2/f_p{}^2)} \tag{20}$$

where

$$f_p = \frac{Z_0}{2\mu_o b} \tag{21}$$

and

$$G = \frac{\pi^2}{12} \frac{[(\epsilon_{e0} - 1) + (b'/b)^2(\epsilon_s - \epsilon_{e0})](\epsilon_{e0} - 1)(\epsilon_s - \epsilon_{e0})}{\epsilon_{e0}(\epsilon_s - 1)^2}. \tag{22}$$

Nonmagnetic substrates are assumed; therefore, $\mu_o = 31.9186$ nH/in. Equation (20) is the final analytical expression for dispersion of microstrip. Investigation of experimental results shows that G approximates unity.

Evaluation of Parameters

Dispersion curves for microstrip lines on alumina substrates 0.025 and 0.050 in thick were measured. The microwave measurements were made on ring resonators [8], and the 1-MHz points were determined from the MSTRIP program by using the value of the substrate dielectric constant ϵ_s found from capacitance measurements of each fully metallized substrate. These data were used to calculate the multiplier of f^2 in (20) that forced a fit at 10 GHz for each microstrip line. Then, values of b'/b were calculated using (21) and (22). The results are shown in Fig. 3, which indicates that $b'/b \simeq 3$ for characteristic impedances above about 35 Ω. The experimentally determined values of G are also plotted in Fig. 3.

Equations (20) and (21) clearly demonstrate the nature of the dependence of the effective dielectric constant on the substrate thickness b and microstrip characteristic impedence Z_0.

In many engineering applications of microstrip, dispersion can be treated as a correction factor to the zero-frequency

effective dielectric constant ϵ_{e0}; thus only approximate values are required. In such situations, it is sufficient to assume that $G=1.0$ in (20). For greater accuracy, the curves in Fig. 3, or an equivalent based on other careful measurements, can be used. A linear approximation of curves of Fig. 3 is

$$G = 0.6 + 0.009\, Z_0. \tag{23}$$

The Inflection Point

Study of the dispersion function (20) can provide some general information about typical dispersive behavior. Equation (20) shows that the effective dielectric constant goes from a value of ϵ_{e0} at zero frequency to a value of ϵ_s at infinite frequency, in agreement with theory [2], and that the slope of ϵ_e with respect to frequency is zero at both extremes. The frequency of the maximum slope between these two points is called the inflection point. The requirement that the second derivative of ϵ_e with respect to frequency must equal zero gives the inflection frequency

$$f_i = \frac{f_p}{\sqrt{3G}}. \tag{24}$$

Using (24) in (20) yields the value of the effective dielectric constant ϵ_{ei} at the inflection frequency:

$$\epsilon_{ei} = \tfrac{1}{4}(\epsilon_s + 3\epsilon_{e0}) \tag{25}$$

and the slope with respect to frequency at ϵ_{ei}:

$$\left.\frac{d\epsilon_e}{df}\right|_{f=f_i} = \tfrac{3}{8}(\epsilon_s - \epsilon_{e0}). \tag{26}$$

A graphical construction that makes it possible to draw a straight line tangent to the inflection point of the dispersion curve has been shown in Fig. 1.

It can be observed that the dispersion and the inflection relationships agree closely with measured data. Equations (24) and (25) do in fact predict the frequency and effective dielectric constant values at which measured dispersion curves have maximum slope, and that slope is in very good agreement with (26) for an ideal dispersion function. This detailed agreement between theory and experiment supports the validity of the LSE model of microstrip propagation.

Comparison with Measurements

The theory developed in this paper will first be compared with the theoretical prediction of Zysman and Varon [2] for a microstrip line having the following characteristics: $\epsilon_s=9.7$, $\epsilon_{e0}=6.50$, $Z_0=50$, and $b=0.05$ in. The unknown parameter G will be found from the inflection point formulas and the graphical data of [2].

Using (25) to calculate the inflection point gives $\epsilon_{ei}=7.3$; [2, fig. 5] then gives $f_i=9$ GHz. Equation (24) predicts

$$\frac{G}{f_p^2} = \frac{1}{3f_i^2} = 0.00412. \tag{27}$$

Using values given above in (21) yields

$$f_p = \frac{Z_0}{2\mu b} = \frac{50}{2 \times 31.92 \times 0.05} = 15.66 \text{ GHz}. \tag{28}$$

Substituting (28) into (27) yields

$$G = 0.00412 \times 15.66^2 = 1.01. \tag{29}$$

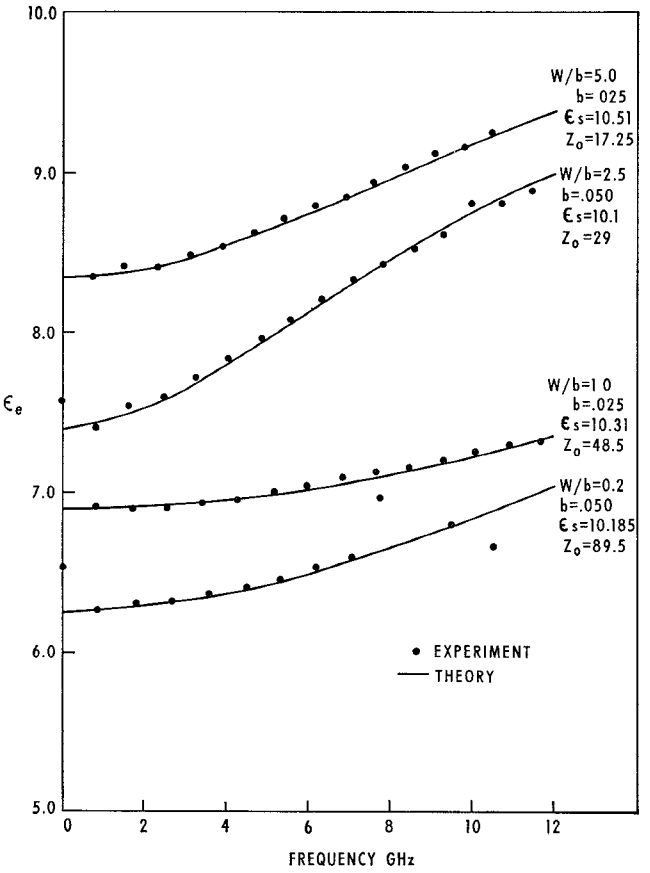

Fig. 4. Comparison of dispersion function and measurements.

This value can be compared with the approximate value $G=1.0$ or the curve-fit formula (23), which gives $G=1.05$.

The next problem is to determine the model parameters of the dispersion measurements on rutile reported by Hartwig *et al.* [1]. The given parameters are $\epsilon_s=104$, $\epsilon_{e0}=62$ (calculated from capacitance measurement), $b=0.05$, and $Z_0=20$ Ω. However, since the dispersion curve must have a zero slope at zero frequency, an extrapolation of the measured points on [1, fig. 3] clearly yields a greater value of ϵ_{e0} than 62. A value of 63.5 will be used in these calculations.

Following the same procedure used in the preceding example gives $\epsilon_{ei}=73.6$ and $f_i \approx 4.4$, so that $G/f_p^2=0.0172$. Equation (21) gives $f_p=6.22$ GHz; thus $G=6.22^2 \times 0.0172 = 0.667$. The approximate formula (23) gives $G=0.78$. Either value of G gives a calculated curve that is within the scatter of the measured points. The first value of G, based on inflection point formulas, seems to average out a little better, however. This is reasonable because it is based in part on the data it characterizes.

The last comparison of theory and experiment is shown in Fig. 4. The solid-line curves were calculated from the dispersion function (20) by using (23) to set the value of G in each case. The round points are values of effective dielectric constant measured at COMSAT Laboratories. The circuits used were ring resonators [8] on commercial 0.025- and 0.05-in alumina substrates. In each case, the value of ϵ_{e0} was found by extrapolating the curve of microwave measurements to zero frequency. Then, curves generated by the MSTRIP program [6] were used to determine a value of ϵ_s for the appropriate width-to-height ratio of the line. The shapes and values of the experimental and theoretical curves are found to be in good agreement.

Limitations and Applications

The basic hypothesis of this paper is that the dispersion function (20) describes the propagation characteristics of any microstrip-like transmission line. So far, measurements on microstrip have supported this point of view.

A more general theoretical investigation than given in this paper would be necessary to explore the fundamental limitations on applying the dispersion function. Some points can be considered, however.

The dispersion relation applies only to the fundamental LSE mode. It probably holds closely only for thin ($b < \lambda/4$ in ϵ_s) substrates and strips that are not very wide ($w < \lambda/3$ in ϵ_s) to insure that the LSE mode is dominant, but these restrictions seldom arise in microstrip applications. Also, the dispersion relation takes on the correct value at infinite frequency, and so there is no clearly defined upper-frequency limit at which it no longer applies. The practical upper-frequency limit of microstrip, where every junction and discontinuity radiate strongly via surface wave modes [1], probably occurs before the dispersion function becomes unreliable.

Since the dispersion function appears to have general applicability to all structures having the same types of boundaries as microstrip and propagating an LSE mode, it would be expected to hold for microstrip with or without an enclosure, for the even and odd modes of the parallel-coupled microstrip, and possibly for other quasi-TEM structures, such as inhomogeneously loaded coaxial line. It would, of course, be necessary to have appropriate values for ϵ_s, ϵ_{e0}, Z_0, and G for each structure.

Acknowledgment

The author wishes to thank Dr. W. J. English for his technical discussions and T. J. Lynch for his careful measurements.

References

[1] C. Hartwig, D. Massé, and R. Pucel, "Frequency dependent behavior of microstrip," in *1968 G-MTT Symp. Dig.*, pp. 110–116.
[2] G. Zysman and D. Varon, "Wave propagation in microstrip transmission lines," in *1969 G-MTT Symp. Dig.*, pp. 3–9.
[3] O. Jain, V. Makios, and W. Chudobiak, "Coupled-mode model of dispersion in microstrip," *Electron. Lett.*, vol. 7, pp. 405–407, July 15, 1971.
[4] M. V. Schneider, "Microstrip dispersion," *Proc. IEEE (Special Issue on Computers in Design)* (Lett.), vol. 60, pp. 144–146, Jan. 1972.
[5] R. Collin, *Field Theory of Guided Waves*. New York: McGraw-Hill, 1960, p. 224.
[6] T. G. Bryant and J. A. Weiss, "MSTRIP (parameters of microstrip)," *IEEE Trans. Microwave Theory Tech.*, vol. MTT-19, pp. 418–419, Apr. 1971.
[7] C. Montgomery, R. Dicke, and E. Purcell, *Principles of Microwave Circuits* (M.I.T. Radiation Laboratory Series), vol. 8. New York: McGraw-Hill, 1948.
[8] P. Troughton, "Measurement techniques in microstrip," *Electron. Lett.*, vol. 5, pp. 25–26, Jan. 23, 1969.

Nonlinear Analysis of the Schottky-Barrier Mixer Diode

DOMINIC A. FLERI AND LEONARD D. COHEN

Abstract—**The waveshape of the local-oscillator voltage component that exists across the nonlinear junction of a Shottky-barrier diode is a fundamental determinant of mixer performance. This waveshape significantly differs from that of the total local-oscillator voltage impressed across the diode terminals since it is influenced by parasitics, particularly spreading resistance and contact inductance, which exist in series with the junction. The junction-voltage waveshapes resulting from a 9.375-GHz sinusoidal local-oscillator generator voltage are computed for three common equivalent-circuit models of the diode. In the first model the diode is represented by a nonlinear conductance in series with a fixed spreading resistance. The second model includes the nonlinear capacitance associated with the junction, and the third additionally includes the contact inductance. In each case, the junction-voltage waveshape is significantly nonsinusoidal. It is shown that the contact inductance can induce a peak inverse junction voltage that greatly exceeds the peak voltage impressed across the diode terminals. This parasitic reactance thus can have an important bearing on the burnout properties of the mixer diode.**

Manuscript received April 24, 1972; revised July 17, 1972.

D. A. Fleri was with the Bayside Research Center, General Telephone and Electronics Laboratories, Incorporated, Bayside, N. Y. 11360. He is now with the Department of Advanced Receiver Components and Subsystems, AIL, a division of Cutler-Hammer, Melville, N. Y.

L. D. Cohen is with the Bayside Research Center, General Telephone and Electronics Laboratories, Incorporated, Bayside, N. Y. 11360.

I. Introduction

OVER THE YEARS, a number of investigators [1]–[6] have published detailed mathematical treatments for determining the performance characteristics of semiconductor diode heterodyne mixers. These techniques basically involve the formulation of an admittance matrix or equivalent set of parameters, which describes the linearized small-signal current–voltage relations that exist among the coupled-signal, image, and intermediate frequency voltage components in the mixer. The admittance matrix facilitates the analytical determination of mixer conversion loss, as well as the associated RF and IF impedances. In general, the matrix elements are functions of both the amplitude and waveshape of the local-oscillator voltage component that exists across the nonlinear junction of the semiconductor diode. This waveshape was assumed to be sinusoidal by the early investigators because it was not practical to derive the exact waveshapes with the computational facilities then available. This assumption has been perpetuated over the years and is retained even in present-day analyses. As was pointed out by Barber [7], however, the actual waveshape of the local-oscillator junction voltage is significantly non-